The Role of Porosity in Filtration

Part X: Deposition of Compressible Cakes on External Radial Surfaces

The theory of deposition of compressible, particulate beds on cylindrical surfaces is developed for both constant-pressure and constant-rate filtration. Radial flow is encountered in tubular filters and in both filtering and sedimenting centrifuges. It differs mathematically from filtration on planar surfaces in the manner in which the frictional drag balance on the particle structure is coupled with Darcy's equation.

F. M. TILLER
and C. S. YEH
Department of Chemical Engineering
University of Houston
Houston, TX 77004

SCOPE

Radial geometry in solid-liquid separation is encountered principally in cakes laid down externally in candle or tubular filters (Figure 1) and internally in centrifuges. Production of a cake on the inside of a spherical filter utilized for high energy batteries represents an example of spherical flow (Bieman, 1984).

Literature related to filtration has almost exclusively been devoted to one-dimensional Cartesian coordinate systems. Whereas solutions for radial flow through a porous cylindrical shell with constant permeability have been available for many years (Bird et al., 1960), only minimal attention has been focused on flow involving compressible cakes (Shirato et al., 1973; Yoshioka et al., 1972). The use of equations for incompressible cakes deposited on cylindrical surfaces leads to gross errors when applied to compressible materials.

The internal mechanisms governing flow and cake compressibility are controlled by the coupled action of the Darcian frictional drag and the resulting collapse of the particulate structure, which in turn affects the local permeability and porosity. In one-dimensional x-coordinate flow, a force balance with the usual simplifying assumptions including point contact leads to (Tiller and Crump, 1977): $dp_L + dp_s = 0$, where p_L is the local liquid (hydraulic) pressure and p_s, termed effective or compressive drag pressure, is the accumulative frictional drag on the particles in the cake between an arbitrary point and the surface. This equation states that the frictional drop of the liquid is offset by a corresponding increase in the effective pressure on the solids. The liquid pressure p_L enters the Darcy equation, and p_s determines the state of the cake structure as reflected in local values of porosity and permeability. In radial flow, Figure 2, the angular component of the effective pressure enters the force balance and leads to the more complicated Eq. 3 relating p_s and p_L. Equation 12, which results from coupling the force balance involving p_s with Darcy's Eq. 4, does not lend itself to the relatively simple solutions encountered in unidimensional, x-coordinate flow processes. Both analytical and numerical solutions are presented for constant-pressure and constant-rate filtration. With slight modifications, the equations can be adapted for use with centrifugal pumps.

CONCLUSIONS AND SIGNIFICANCE

Equations derived in this paper provide relationships for calculating porosity and liquid presure as functions of distance through the cake. Application of boundary conditions dependent on the pumping mechanism and the supporting medium permits determination of the flow rate (Figure 8) and average porosity (Figure 9) as functions of applied pressure. Cakes with high compressibility do not respond well to increasing pressure. The flow rate reacts sluggishly when pressure is increased. With the most compressible material shown in Figure 8, the flow rate is roughly proportional to the 0.2 power of the pressure drop across the cake. Thus pressure has diminishing value as the compressibility increases.

In conventional cakes formed on a plane surface, the increase in effective pressure p_s (accumulative drag on the particles) equals the drop in pressure Δp_c across the cake. Average values of porosity and flow resistance (or permeability) are then unique functions of the liquid pressure drop across the cake Δp_c which equals $(-\Delta p_s)$. However, in radial flow, growth in surface area leads to an increasing total stress on the cake surface. Part of the stress is absorbed in bridging action of the particles

(equivalent to the lateral stress in soils), and the remainder is transmitted to the medium. As the cake grows, the effective stress on the solids at the medium increases. Unlike x-coordinate flow, the liquid pressure drop across the cake does not equal the increase in the effective stress ($-\Delta p_s$). As the effective pressure p_s determines local values of porosity and permeability, average values of flow resistance α_{av} and permeability K_{av} are a function of both the manner in which p_s varies and the limit at the medium. Thus α_{av} and K_{av} are not unique functions of Δp_c as in planar cakes.

In conventional constant-pressure filtration with negligible cake resistance, the porosity and liquid pressure are unique functions of the fractional distance through the cake. In radial flow, the variation of porosity and liquid pressure with fractional distance changes with cake thickness.

RADIAL FILTRATION THEORY

In a tubular filter, Figure 1, flow is directed radially inward toward the origin. As the cake grows, the total force exerted at the cake surface in a constant-pressure filtration increases linearly with the increasing cake radius. In contrast to cakes produced on planar surfaces (leaf filters, and plate and frame presses), the force transmitted through the cake to the medium grows with time because of the increasing surface area. Radial filtration also differs from planar filtration in that the liquid velocity increases as the radius decreases.

In the first stage of development of the theory, differential momentum and continuity balances will be combined with the Darcy rate equation in spatial coordinate form. After assuming quasisteady state and constant flow rate throughout the cake (slow cake compression), the differential equations will be integrated to yield the pressure and porosity variations across the cake. It will be assumed that the instantaneous relationships among cake thickness, flow rate, and pressure profile are independent of past history. The second step involves application of boundary conditions developed by the pumping mechanism and determination of volume of filtrate as a function of time.

We begin by assuming that momentum changes due to liquid flow and solid movement are negligible. Then a simple free body force balance suffices for relating frictional drag to stress on the particulate bed, as pictured in Figure 2. As liquid flows through the cake, we use the term "hydraulic pressure" in reference to the driving force appearing in the Darcy-Shirato Eq. 4. The stress developed in the solid is assumed to act as in soils, with the ratio of the lateral to radial stress being constant and equal to the coefficient of earth pressure at rest, k_o (Brooker and Ireland, 1965). The total internal force, F_s, is assumed from a macroscopic standpoint to be uniformly distributed around the radius, r. Point contact among particles is assumed so that the liquid pressure is active over the entire surface of each particle. Then we define the effective pressure

$$p_s = F_s/2\pi r \tag{1}$$

where F_s has the dimensions of force per unit height. Referring to Figure 2, we now write a force balance in the form

$$d(rp_L)d\theta + d(rp_s)d\theta = (p_L + k_o p_s)dr \sin(d\theta). \tag{2}$$

With $d\theta = \sin(d\theta)$, Eq. 2 reduces to

$$\frac{dp_L}{dr} + \frac{dp_s}{dr} + (1 - k_o)\frac{p_s}{r} = 0 \tag{3}$$

The p_L term cancels on each side because the hydraulic pressure is isotropic. The effective pressure term remains because k_o is not unity. Reported values for k_o vary from 0.3 to 1.0. Tiller and Lu (1972) obtained values of 0.45 and 0.34, respectively, for sand and Solka Floc.

The Darcy-Shirato equation assumes that the pressure gradient

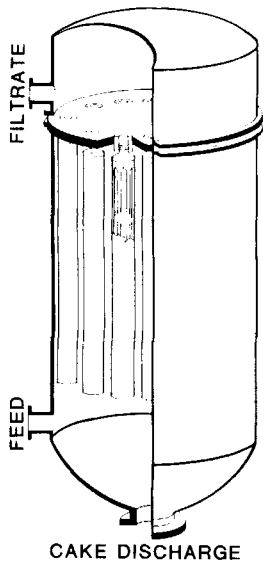

Figure 1. Example of tubular or candle filter (Purchas, 1981).

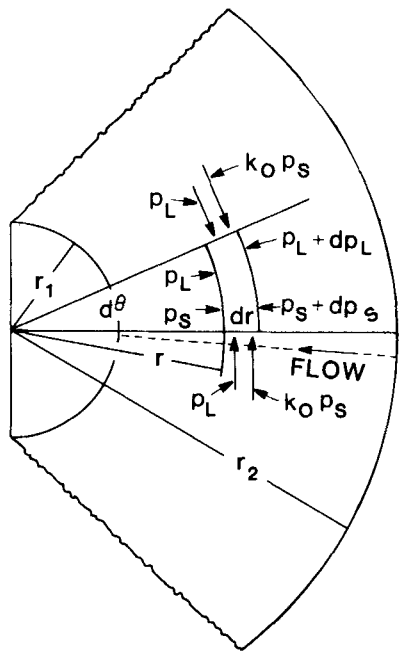

Figure 2. Liquid and solid compressive pressures in radial flow.

is related to the difference in velocities of liquid and solid as follows:

$$\frac{dp_L}{dr} = \frac{\mu\epsilon}{K}(u_L - u_s) = \frac{\mu\epsilon}{2\pi rK}\left(\frac{Q}{\epsilon} - \frac{Q_s}{1-\epsilon}\right) \tag{4}$$

where Q and Q_s have dimensions of volume/(time)(height).

Although the solids are in motion because of continuous compression of the cake, the solid velocity term is only of importance for filtration of highly concentrated slurries where the rate of cake buildup is rapid, i.e., growth rates of 10–50 mm/min prevail, with total filtration time measured in seconds. In expression operations, the solid velocity term is of prime importance, as the average velocities of liquid and solid are equal because the solid displaces an equal volume of liquid. Our slurries will be relatively dilute, with slow cake buildup rates, and the solid velocity term will be omitted.

We next turn to material balances. Both external and internal balances are required for generalized theoretical developments. The external or overall mass balance will be postponed until boundary conditions are introduced. An internal balance involves the continual structural rearrangement of the cake as fluid drag moves individual particles in spurts and jerks toward the medium. Microscopic movements of particulates are the result of continuing failures of local structures. As each solid particle changes position in its movement toward the medium, it displaces liquid at the local level.

A general continuity equation for the liquid involves squeezing of the cake. The liquid contained in an internal portion of the cake lying between an arbitrary radius r and r_1, the radius of the tubular element, is given by

$$\text{Volume of liquid/height} = 2\pi \int_{r_1}^{r} \epsilon r dr \tag{5}$$

where ϵ is the porosity.

The rate of liquid flow Q at r minus the rate Q_1 at r_1 equals the rate of accumulation of liquid or

$$Q - Q_1 = \frac{\partial}{\partial t}\left[2\pi \int_{r_1}^{r} \epsilon r dr\right] = 2\pi \int_{r_1}^{r} \frac{\partial \epsilon}{\partial t} r dr \tag{6}$$

where $Q = Q(r,t)$ and $Q_1 = Q_1(t)$. Differentiating with respect to r yields

$$\frac{\partial Q}{\partial r} = 2\pi r \frac{\partial \epsilon}{\partial t} \tag{7}$$

The porosity at a fixed spatial coordinate decreases with time because of cake compaction; consequently $\partial\epsilon/\partial t < 0$ and Q increases as r decreases from the cake radius r_2 to r_1. However, in our case we assume that $\partial\epsilon/\partial t$ is small and Q is independent of r. A variation of no more than 1–2% should be expected. After obtaining formulas for porosity as a function of r and t, the magnitude of $\partial\epsilon/\partial t$ can be calculated.

Assumption of constant Q throughout the cake at an arbitrary time t leads to ordinary rather than partial differential equations and considerably simplifies the required numerical calculations.

Equations of state relating drag forces to parameters defining the cake structure are required. Conventionally, it is assumed that porosity ϵ and permeability K (or specific flow resistance α) are functions of the initial values ϵ_o and K_o for an unstressed cake and the effective pressure p_s in the form $K = K_o f(p_s)$ where $f(0) = 1$ and $dK/dp_s < 0$. In addition, cake compression is considered to be irreversible (a slight spring-back actually exists), and ϵ and K are determined by the maximum value of p_s reached at any specific location. Tiller and Cooper (1962) proposed the equivalent of the following equations to relate K and ϵ to p_s:

$$\begin{aligned} &p_s \geq p_{si} \quad p_s \leq p_{si} \\ &K = Hp_s^{-\delta} \quad K = K_i = Hp_{si}^{-\delta} \end{aligned} \tag{8}$$

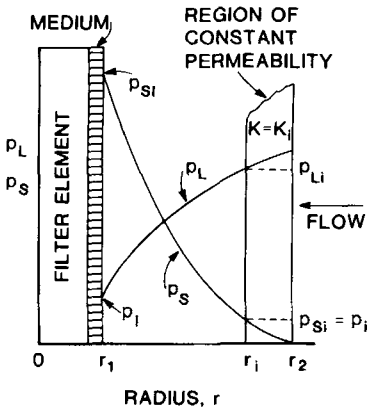

Figure 3. Schematic view of p_s and p_L variation in a radially deposited cake.

$$\epsilon_s = 1 - \epsilon = Bp_s^{\beta} \quad \epsilon_{si} = 1 - \epsilon_i = Bp_{si}^{\beta} \tag{9}$$

Tiller and Leu (1980) discussed the relative merits of Eqs. 8 and 9 and a new set of equations having the form

$$K = K_o(1 + p_s/p_a)^{-\delta} \tag{10}$$

$$1 - \epsilon = (1 - \epsilon_o)(1 + p_s/p_a)^{\beta} \tag{11}$$

These equations possess the advantage of incorporating the unstressed parameters K_o and $(1 - \epsilon_o)$, whereas H and B are simply empirical constants. Graphical methods for obtaining the parameters in Eqs. 8–11 were presented by Tiller and Leu (1980). For a given cake, the values of β and δ obtained from Eqs. 8 and 9 differ somewhat from those appearing in Eqs. 10 and 11.

In the absence of substantial quantities of data, we shall assume that the form of Eqs. 8–11 which have been employed extensively in one-dimensional, rectangular coordinate flow can be used for radial flow. For identical values of p_s in radial and rectangular flow, we assume that K and ϵ are the same for the two cases.

PRESSURE AS A FUNCTION OF RADIUS

We shall first obtain equations relating the compressive drag and hydraulic pressure to the radius. This procedure will provide a relation between the instantaneous flow rate, cake thickness, and applied pressure. On the basis of a quasisteady-state assumption that the instantaneous conditions are independent of prior history, volume will be obtained as a function of time. We neglect the solid velocity in the Darcy-Shirato equation and combine it with Eq. 3 to give the general differential equation for radial filtration (Shirato and Aragaki, 1969)

$$\frac{dp_s}{dr} + (1 - k_o)\frac{p_s}{r} = -\frac{\mu Q}{2\pi rK} = -\frac{dp_L}{dr}. \tag{12}$$

The portion of this equation involving p_s and r determines the structure of the cake and the local values of porosity and permeability. The remaining portion containing p_L and r provides information from which rates of flow are obtained. The permeability is assumed to follow Eq. 8. Inasmuch as K takes different forms for p_s greater or less than p_{si}, two sets of equations result. Nomenclature governing the two regions is shown in Figure 3. As long as $p_s \leq p_{si}$, we assume that the permeability is constant and $K = K_i = Hp_i^{-\delta}$. The liquid pressure falls to p_{Li} in this region and is approximately equal to $p - p_{si}$. For moderately compressible materials, i.e., $\delta < 0.6$, the constant permeability region can be neglected. However, for highly compressible cakes, the region from r_i to r_2 is significant.

We first solve Eq. 12 for p_s as a function of r. With the effective pressure distribution known, local and average values of porosity and permeability can be calculated. After the formula for p_s is substituted into Eq. 12, a relation between liquid pressure and radius results. Ultimately the instantaneous flow rate is obtained as a function of the liquid pressure drop.

The value of the permeability as given by Eq. 8 is substituted into Eq. 12, and the variables are separated to produce

$$-(1-k_o)\frac{dr}{r} = \frac{dp_s}{p_s + G(p_s/p_{si})^{\delta}} = \left[\frac{1}{p_s} - \frac{Gp_{si}{}^{-\delta}p_s{}^{\delta-2}}{1 + Gp_{si}{}^{-\delta}p_s{}^{\delta-1}}\right]dp_s \tag{13}$$

where

$$G = \mu Q/2\pi K_i(1-k_o) \tag{14}$$

We shall integrate Eq. 12 in the region in which $K = K_i$ and $r_i \le r \le r_2$. Next Eq. 13 will be integrated in the portion of the cake for which $r_1 \le r \le r_i$. The former yields

$$\left(\frac{r_2}{r_i}\right)^{1-k_o} = \frac{p_{si} + G}{G} \tag{15}$$

and the latter is

$$\left(\frac{r_i}{r}\right)^{(1-k_o)(1-\delta)} = \frac{p_s^{1-\delta}p_{si}^{\delta} + G}{p_{si} + G} \tag{16}$$

Eliminating r_i between Eqs. 15 and 16 leads to

$$\left(\frac{r_2}{r}\right)^{(1-k_o)(1-\delta)} = \left(\frac{p_{si} + G}{G}\right)^{1-\delta}\left(\frac{p_s^{1-\delta}p_{si}^{\delta} + G}{p_{si} + G}\right) \tag{17}$$

Solving for p_s gives

$$p_s^{1-\delta} = \left(\frac{r_2}{r}\right)^{(1-k_o)(1-\delta)}\left(\frac{G}{p_{si} + G}\right)^{1-\delta} \times \left[p_{si}^{1-\delta} + \frac{\mu Q}{2\pi H(1-k_0)}\right] - \frac{\mu Q}{2\pi H(1-k_o)} \tag{18}$$

$$= J\left(\frac{r_2}{r}\right)^{(1-k_o)(1-\delta)} - \frac{\mu Q}{2\pi H(1-k_o)} \tag{19}$$

In order to obtain the p_L distribution, Eq. 19 is substituted into Eq. 12 to produce

$$dp_L = \frac{\mu Q}{2\pi H}\left[J\left(\frac{r_2}{r}\right)^{(1-k_o)(1-\delta)} - \frac{\mu Q}{2\pi H(1-k_0)}\right]^{\delta/(1-\delta)}\frac{dr}{r} \tag{20}$$

In the region in which the permeability is assumed constant, Eq. 20 reduces to

$$dp_L = (1-k_o)G\,dr/r \tag{21}$$

which is equivalent to the equation for an incompressible cake. Integrating Eq. 21 from the applied pump pressure p to p_{Li} and r_2 to r_i leads to

$$p - p_{Li} = \frac{\mu Q}{2\pi K_i}\ln\frac{r_2}{r_i} \tag{22}$$

For an incompressible solid, p_{Li} and r_i can be replaced p_1 and r_1. The hydraulic pressure is obtained by integrating Eq. 12 to give

$$p_{Li} = p - G\ln\left(1 + \frac{p_{si}}{G}\right) \tag{23}$$

These values of p_{Li} and r_i will be used as integration limits for the cake lying between r_1 and r_i. We shall return to these equations to complete the derivation for flow through an incompressible cake in the next section.

Integrating Eq. 20 between the limits (p_1, r_1) and (p_{Li}, r_i) and eliminating p_{Li} by means of Eq. 23 gives

$$p_{Li} - p_1 = p - G\ln\left(1 + \frac{p_{si}}{G}\right) - \frac{\mu Q}{2\pi r_1}R_m = \frac{\mu Q}{2\pi H}\int_{r_1}^{r_i}\left[J\left(\frac{r_2}{r}\right)^m - \frac{\mu Q}{2\pi H(1-k_0)}\right]^{\delta/(1-\delta)}\frac{dr}{r} \tag{24}$$

where R_m is the medium resistance. Numerical integration is required for solution of this equation in general. Nevertheless, there are several practical values of δ (0.5, 2/3, 0.75, 0.8, 1.0, etc.) for which analytical solutions are available. A value of $\delta = 0.5$ corresponds to a moderately compressible cake and therefore is of interest. For values of δ less than approximately 0.5–0.6, the term in p_{si} may be neglected, leading to a more simple expression. Placing $p_{si} = 0$ leads to $J = \mu Q/2\pi H(1-k_o)$ in Eq. 24, and the following equation results

$$p = \frac{\mu Q R_m}{2\pi r_1} + \left(\frac{1}{1-k_o}\right)^{\delta/(1-\delta)}\left(\frac{\mu Q}{2\pi H}\right)^{1/(1-\delta)} \times \int_{r_1}^{r_2}\left[\left(\frac{r_2}{r}\right)^m - 1\right]^{\delta/(1-\delta)}\frac{dr}{r} \tag{25}$$

For the special case in which $\delta = 0.5$ and $k_o = 0.5$, Eq. 25 reduces to

$$p = \frac{\mu Q R_m}{2\pi r_1} + 2\left(\frac{\mu Q}{2\pi H}\right)^2\int_{r_1}^{r_2}\left[\left(\frac{r_2}{r}\right)^{1/4} - 1\right]\frac{dr}{r} \tag{26}$$

Integration yields

$$p = \frac{\mu Q R_m}{2\pi r_1} + \frac{1}{2}\left(\frac{\mu Q}{\pi H}\right)^2\left\{4\left[\left(\frac{r_2}{r_1}\right)^{1/4} - 1\right] - \ln\frac{r_2}{r_1}\right\} \tag{27}$$

The dimensions of H in this equation are the same as $Kp^{1/2}$, thus accounting for the apparent problem of units of the Q and Q^2 terms. Solving for $\mu Q/\pi H$

$$\frac{\mu Q}{\pi H} = \frac{-\frac{HR_m}{2r_1} + \left\{\left(\frac{HR_m}{2r_1}\right)^2 + 2p\left[4\left(\frac{r_2}{r_1}\right)^{1/4} - 4 - \ln\left(\frac{r_2}{r_1}\right)\right]\right\}^{1/2}}{4\left(\frac{r_2}{r_1}\right)^{1/4} - 4 - \ln\left(\frac{r_2}{r_1}\right)} \tag{28}$$

For negligible medium resistance, Eq. 28 becomes

$$\frac{\mu Q}{\pi H} = \left[\frac{2p}{4\left(\frac{r_2}{r_1}\right)^{1/4} - 4 - \ln\left(\frac{r_2}{r_1}\right)}\right]^{1/2} \tag{29}$$

Although analytical equations can be obtained for other special values, they will not be given here.

Equation 22 can be adapted for incompressible solids by substituting $p_1 = p_{Li}$ and $r_i = r_1$ to produce

$$p = \frac{\mu Q}{2\pi r_1}\left[\frac{r_1}{K}\ln\left(\frac{r_2}{r_1}\right) + R_m\right] \tag{30}$$

Equations 25–30 provide a series of relationships which represent an instantaneous view of flow through a cake of fixed thickness under a given pressure drop. Our next task consists of finding formulas relating time to volume filtered and cake thickness. Material balances are required to relate the volumes and masses of slurry, cake, and filtrate.

MATERIAL BALANCES

Inasmuch as p_s can be obtained as a function of r through use of Eq. 19, the volume fraction of solids, $\epsilon_s = 1 - \epsilon$, can be calculated at various distances through the cake. The volume-averaged solid fraction is given by

$$\epsilon_{sav} = \frac{2\pi \int_{r_1}^{r_2} \epsilon_s r dr}{\pi(r_2^2 - r_1^2)} = \frac{2}{r_2^2 - r_1^2} \times \left[\int_{r_1}^{r_i} \epsilon_s r dr + \epsilon_{si} \int_{r_i}^{r_2} r dr\right] \quad (31)$$

A total material balance on a volumetric basis gives

$$\text{vol. of slurry} = \text{vol. of cake} + \text{vol. of filtrate}$$

$$\frac{\omega_c}{\phi_s} = \frac{\omega_c}{\epsilon_{sav}} + v \quad (32)$$

where ω_c and v are respectively volumes of cake solids and filtrate/unit area of the medium and ϕ_s equals the volume fraction of solids in the slurry. We also have

$$\omega_c = \epsilon_{sav}(r_2^2 - r_1^2)/2r_1 \quad (33)$$

Solving for v with Eqs. 32 and 33 leads to

$$v = \frac{\epsilon_{sav} - \phi_s}{\phi_s}\left(\frac{r_2^2 - r_1^2}{2r_1}\right) \quad (34)$$

The filtration rate Q must be related to the rate of change of r_2. Differentiating Eq. 34 yields

$$\frac{Q}{2\pi r_1} = \frac{dv}{dt} = \frac{\epsilon_{sav} - \phi_s}{\phi_s}\frac{r_2}{r_1}\frac{dr_2}{dt} + \frac{1}{\phi_s}\left(\frac{r_2^2 - r_1^2}{2r_1}\right)\frac{d\epsilon_{sav}}{dt} \quad (35)$$

For most filtrations the rate of variation of ϵ_{sav} with time is small (see Figure 7), and the last term can be neglected.

Elimination of p_s between Eqs. 9 and 19 results in a relation of ϵ_s to r; thus

$$\epsilon_s = B\left[J\left(\frac{r_2}{r}\right)^m - \frac{\mu Q}{2\pi H(1 - k_o)}\right]^{\beta/(1-\delta)} \quad (36)$$

Substituting in Eq. 31, integrating the last term, and eliminating r_i utilizing Eq. 15 yields

$$\epsilon_{sav} = \frac{2}{r_2^2 - r_1^2}\left\{B\int_{r_1}^{r_i}\left[J\left(\frac{r_2}{r}\right)^m - \frac{\mu Q}{2\pi H(1 - k_o)}\right]^{\beta/(1-\delta)} r dr + \frac{\epsilon_{si} r_2^2}{2}\left[1 - \left(\frac{G}{G + P_{si}}\right)^{2/(1-k_o)}\right]\right\} \quad (37)$$

For moderately compressible materials where $r_i \approx r_2$ and $p_{si} \approx 0$, Eq. 37 reduces to

$$\epsilon_{sav} = \frac{2B\left[\frac{\mu Q}{2\pi H(1 - k_o)}\right]^{\beta/(1-\delta)}}{r_2^2 - r_1^2} \times \int_{r_1}^{r_2}\left[\left(\frac{r_2}{r}\right)^m - 1\right]^{\beta/(1-\delta)} r dr \quad (38)$$

TIME RELATIONSHIPS

In order to obtain filtrate volume or cake volume as a function of time, the relationship between p and Q as determined by the pumping mechanism must be known. In general, constant-pressure (usually vacuum), constant-rate, and centrifugal pump operations are utilized in filtration. Equation 24 provides a general relationship among p, Q, and r_2 while Eqs. 26–30 represent various special cases. When an integration is required, Q is replaced by Eq. 35.

Constant-Rate Filtration

Equation 24 serves as a basis for constant rate filtration with Q held constant. Normally the volume of filtrate V is placed equal to Qt, i.e. $V = Qt$, where Q equals the pump output. Utilizing Eq. 34, the r_2 vs. time relation can be written in the form

$$V = Qt = \frac{\epsilon_{sav} - \phi_s}{\phi_s}\pi(r_2^2 - r_1^2) \quad (39)$$

The radius of the cake is related to t by

$$r_2 = \left[r_1^2 + \frac{\phi_s Q t}{\pi(\epsilon_{sav} - \phi_s)}\right]^{1/2} \quad (40)$$

This value of r_2 is used as the upper limit of Eq. 24 or is substituted into Eqs. 27–29. As an example, we select Eq. 29 with $\delta = 0.5$ and solve for p

$$p = \frac{1}{2}\left(\frac{\mu Q}{\pi H}\right)^2\left\{4\left[1 + \frac{\phi_s Q t}{\pi r_1^2(\epsilon_{sav} - \phi_s)}\right]^{1/8} - 4 - \frac{1}{2}\ln\left[1 + \frac{\phi_s Q t}{\pi r_1^2(\epsilon_{sav} - \phi_s)}\right]\right\} \quad (41)$$

This equation provides a relationship between p and t for constant rate filtration.

Constant-Pressure Filtration

If the pressure is constant, Q varies, and an integration on r_2 is required. Analytical formulas can only be obtained for the incompressible case (Shirato et al., 1968). Filtration time t is calculated by means of

$$t = \int_0^V dV/Q \quad (42)$$

Numerical integration of Eq. 42 requires that Q be known as a function of V. Various values of r_2 are chosen in any of Eqs. 24–29, and the corresponding values of Q are calculated. The value of V is obtained from Eq. 39. Finally t is found using Eq. 42.

INCOMPRESSIBLE CAKE

For a constant-rate filtration, r_2 from Eq. 40 is substituted into Eq. 30 to give

$$p = \frac{\mu Q}{2\pi r_1}\left\{\frac{r_1}{2K}\ln\left[1 + \frac{\phi_s Q T}{\pi r_1^2(\epsilon_{sav} - \phi_s)}\right] + R_m\right\} \quad (43)$$

For a constant-pressure filtration, we eliminate Q between Eqs. 30 and 35 to obtain

$$\frac{p}{\mu} = \Omega\frac{r_2}{r_1}\frac{dr_2}{dt}\left(\frac{r_1}{K}\ln\frac{r_2}{r_1} + R_m\right) \quad (44)$$

where $\Omega = (\epsilon_{sav}/\phi_s - 1)$. Integrating Eq. 44 with the initial condition $r_2 = r_1$ at $t = 0$ yields

$$\frac{2Kpt}{\Omega\mu r_1^2} = \left(\frac{r_2}{r_1}\right)^2\ln\frac{r_2}{r_1} - \left(\frac{1}{2} - \frac{KR_m}{r_1}\right)\left[\left(\frac{r_2}{r_1}\right)^2 - 1\right] \quad (45)$$

Inasmuch as it is customary to measure the filtrate volume rather than the cake radius, we eliminate r_2 from Eq. 45 in favor of v, volume/unit area of the medium with the help of Eq. 34 to produce

$$\frac{2Kpt}{\Omega\mu r_1^2} = \frac{1}{2}\left(\frac{2v}{\Omega r_1} + 1\right)\ln\left(\frac{2v}{\Omega r_1} + 1\right) - \left(\frac{1}{2} - \frac{KR_m}{r_1}\right)\frac{2v}{\Omega r_1} \quad (46)$$

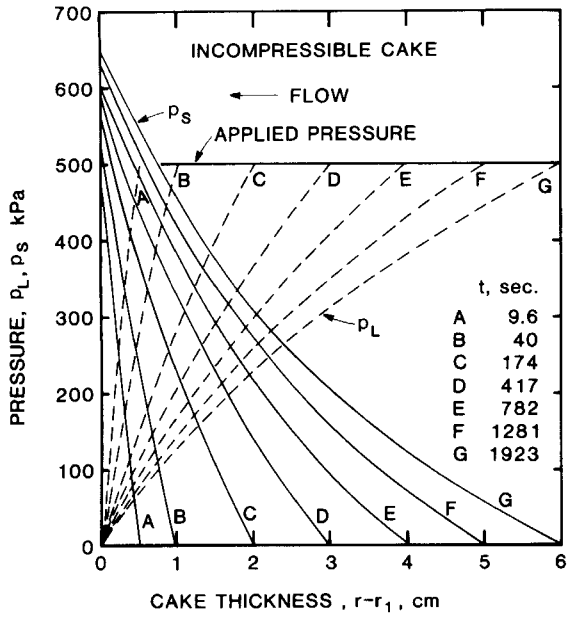

Figure 4. Variation of effective compressive pressure p_s and hydraulic pressure p_L with cake thickness for an incompressible cake.

p = 500 kPa, ϕ_s = 0.02, r_1 = 3.175 cm, μ = 1.0 mPa.s, $H = 10^{-14}$ m², p_{si} = 5 kPa, R_m = 0.

The comparable equation for one-dimensional flow on a flat surface is

$$\frac{2Kpt}{\Omega\mu} = \frac{v^2}{\Omega^2} + \frac{2KR_m}{\Omega}v \tag{47}$$

In the initial period of radial filtration, when v is small, the thin radial cake behaves like a flat cake. When v is small or $2v/\Omega r_1 \ll 1$, $\ln(1 + 2v/\Omega r_1)$ can be approximated by $2v/\Omega r_1 - 0.5(2v/\Omega r_1)^2$. Substituting this approximation into Eq. 46 and neglecting the third-order term in v reduces Eq. 46 to Eq. 47 as expected.

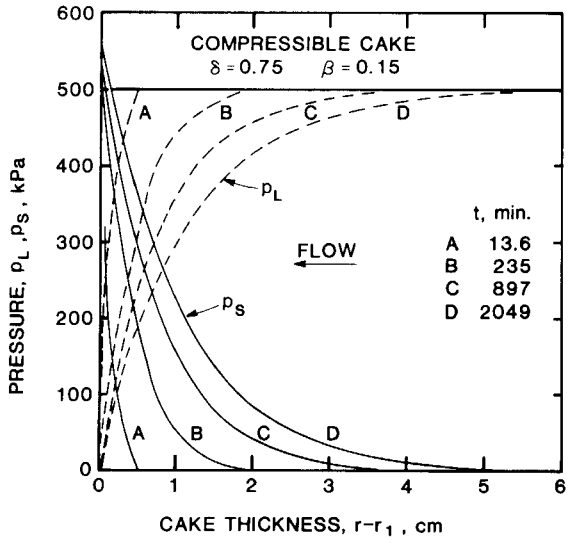

Figure 5. Variation of effective compressive pressure p_s and hydraulic pressure p_L with cake thickness for a moderately compressible cake; conditions as in Fig. 4, except $R_m = 10^{11}$ m^{-1}.

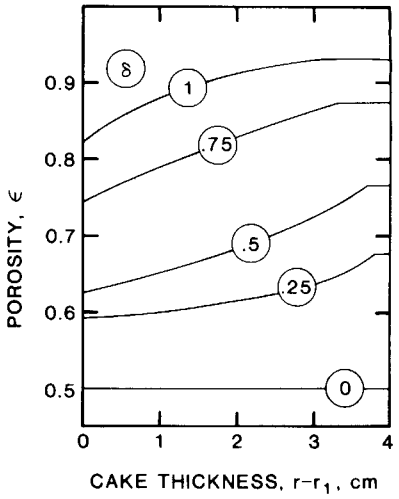

Figure 6. Local porosity as a function of distance through the cake for different compressibilities; conditions as in Fig. 4, except $R_m = 10^{11}$ m^{-1}. B = 0.05, 0.1, 0.2, 0.3, 0.5 starting with the top curve, $\beta = 0.2\,\delta$.

PRESSURE DISTRIBUTION

The distribution of effective pressure within a cake is fundamental to an understanding of its structural features and behavior. In Figures 4 and 5, the effect of compressibility on p_L and p_s pressure distributions is illustrated for different cake thicknesses under a constant applied pressure of 500 kPa. The medium resistance is neglected, and the coefficient of earth pressure is given a value of $k_o = 0.5$. The materials in Figures 4 and 5 are respectively incompressible and moderately compressible. The pronounced curvature of the pressure distributions for the compressible cake in Figure 5 as compared to the smaller curvature for the incompressible material is apparent. Following the dotted p_L curve marked D in Figure 5, it can be seen that the liquid pressure drops 20% to 400 kPa in passing from r = 6.0 cm to 2.0 cm. Then 80% of the pressure drop occurs in the last 2.0 cm, or one-third of the total thickness. The mass of cake in the last 2.0 cm is about 20% of the total. Thus one-fifth of the mass accounts for four-fifths of the pressure drop.

The p_s curve shows similar tendencies. The effective pressure for the 6.0 cm cake rises to about 35 kPa halfway through the cake, which is about 6% of the total increase in p_s. In the 2.0 cm next to the media containing 20% of the cake mass, almost 90% of the in-

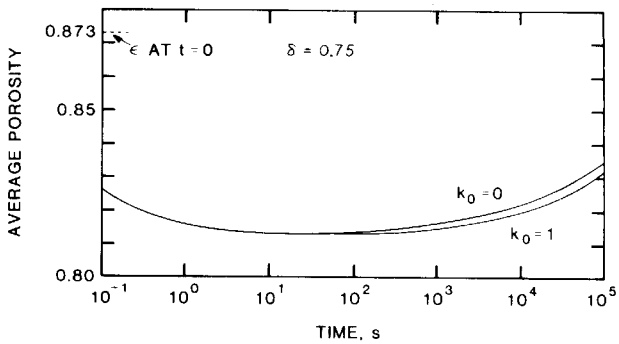

Figure 7. Average porosity as a function of time for δ = 0.75; conditions as in Fig. 5.

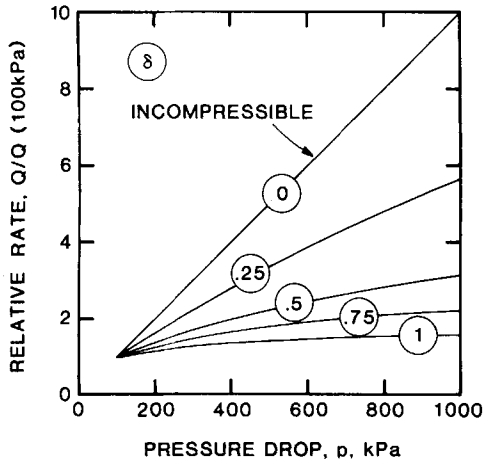

Figure 8. Flow rate vs. pressure drop for different values of compressibility; conditions as in Fig. 4.

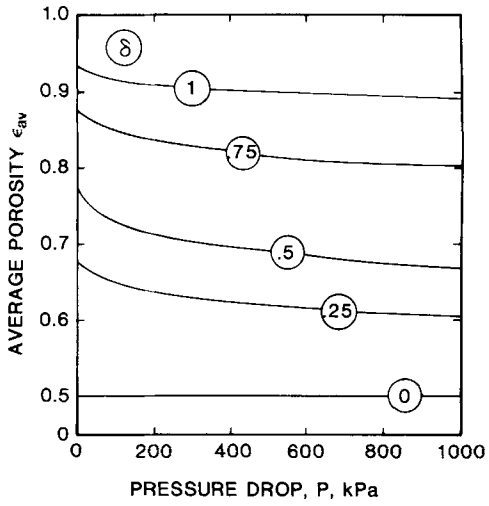

Figure 9. Average porosity vs. pressure drop for different values of compressibility; conditions as in Fig. 6.

crease in p_s occurs. Thus a highly resistant layer or skin is formed near the medium. The remaining part of the cake is more porous and offers comparatively less resistance to flow. The dense "skin" acts adversely on flow rates and hinders the rate of cake growth.

Porosity

In Figure 6, the local porosity is shown as a function of distance through 4.0 cm cakes for different values of ϵ_o and compressibility. The local porosity varies from a maximum at the cake surface to a minimum at the medium, where p_s reaches its maximum. Beginning with an incompressible material in Figure 6, the porosity curves change from a concave downward shape to a convex shape as compressibility increases. The cakes tend to have a much more compact structure at the medium in comparison to a relatively loose condition at the surface.

In Figure 7, the change of average porosity with time is illustrated for the compressible material shown in Figure 5. Calculations for values of k_o = 0, 0.5, 1.0 indicate that large changes in the coefficient of earth pressure have little effect on the cake structure. The average porosity drops at first and then increases with time, in contrast to filtration on a flat surface where it theoretically remains constant when the pressure drop across the cake is constant. The change in average porosity is small and could be considered as constant for most practical operations.

Flow Rate vs. Pressure

Equation 28 provides a relationship for the instantaneous flow rate Q as a function of p for a given cake thickness $(r_2 - r_1)$ when $\delta = 0.5$. Elimination of r_i and p_{Li} among Eqs. 15, 22, and 24 yields an expression in integral form involving Q, p, and r_2 for an arbitrary value of δ. The relative flow rate Q/Q (100 kPa) is illustrated in Figure 8 for various values of compressibility. For an incompressible cake, the flow rate at a given thickness is directly proportional to the pressure drop. In the moderately compressible range of δ up to 0.5, the rate is very nearly proportional to $\Delta p_c^{\,1-\delta}$. Manipulation of Eqs. 25, 28, and 29 indicates that theoretically the ratio of the rates is independent of thickness in the range of moderate compressibility. Numerical calculations indicate that the same relationship continues to hold in the more compressible range. However, as n increases, the effect of pressure on rate diminishes. When $\delta = 1$, the flow rate is approximately proportional to $\Delta p_c^{0.2}$ at moderate pressure drops. As δ and Δp_c become larger, the resistance of the dense layer close to the medium grows. For very high compressibilities, the rate levels off after a moderate Δp_c is reached, and the rate tends to remain constant.

Average Porosity vs. Pressure Drop

In Figure 9 the effect of pressure drop on the average porosity is shown. As pressure increases it has a decreasing effectiveness in reducing the average liquid content. Although large decreases of porosity with pressure might be expected to occur with the most compressible cake, the drop in porosity is modest. The adverse behavior of the highly compressible cake to increasing pressure with respect to both average porosity and flow rate is due to the action of the compressed layer close to the medium.

ACKNOWLEDGMENT

The authors wish to express their appreciation to the National Science Foundation for support which made this research possible under Grant CPE-79-10,590.

NOTATION

B = empirical constant in the equation $1 - \epsilon = Bp_s^{\beta}$, dimensions meaningless
F_s = accumulated drag force on solid per unit height, N/m
G = $G = \mu Q/2\pi K_i(1 - k_o)$, Pa
H = empirical constant in the equation $K = Hp_s^{-\delta}$, dimensions meaningless
J = Eq. 19, dimensions meaningless
K = permeability, m^2
K_o = permeability of unstressed cake, m^2
K_i = permeability when $p_s \leq p_{si}$, m^2
k_o = earth stress ratio
m = $m = (1 - \delta)(1 - k_o)$
n = $n = \delta - \beta$
p = filtration pressure, Pa
p_a = empirical constant in Eqs. 10 and 11, Pa
p_L = hydraulic pressure, Pa
p_{Li} = hydraulic pressure corresponding to $p_s = p_{si}$, Pa
p_s = compressive or effective pressure, Pa
p_{si} = value of p_s below which K and ϵ are assumed constant, Pa
p_{sm} = compressive pressure at interface of medium and cake, Pa

p_1 = hydraulic pressure at interface of medium and cake, Pa
Δp_c = hydraulic pressure drop across cake, Pa
Δp_s = increase in effective pressure across cake, Pa
Q = overall volumetric flow rate of liquid per unit height, $m^3/m \cdot s$
Q_s = overall volumetric flow rate of solids per unit height $m^3/m \cdot s$
Q_1 = overall volumetric flow rate of filtrate per unit height, $m^3/m \cdot s$
R_m = medium resistance, 1/m
r = radius, m
r_i = radius at which $p_s = p_{st}$, m
r_1 = radius of tubular element, m
r_2 = radius of cake surface, m
t = time, s
u_L = true liquid velocity, m/s
u_s = true solid velocity, m/s
V = volume of filtrate per unit height, m^3/m
v = volume of filtrate per unit medium area, m^3/m^2

Greek Letters

α = local specific cake resistance, m/kg
β = empirical constant in Eqs. 9 and 11
δ = empirical constant in Eqs. 8 and 10
ϵ = local porosity
ϵ_s = volume fraction of solids in cake
ϵ_{st} = volume fraction of solids in cake when $p_s \leq p_{st}$
ϵ_{sav} = average solid volume fraction
θ = cylindrical coordiante in the tangential direction
μ = viscosity of liquid, $Pa \cdot s$
ϕ_s = volume fraction of solids in the slurry
ω_c = volume of cake solids per unit medium area, m^3/m^2
Ω = $\epsilon_{sav}/\phi_s - 1$

LITERATURE CITED

Bieman, Leonard, F. M. Tiller, and C. S. Yeh, "Analysis of Filter Cake Formation in Spherical and Linear Geometries," submitted to *Ind. Eng. Chem.* (1984).

Bird, R. B., W. E. Stewart, and E. N. Lightfoot, *Transport Phenomena*, Wiley, New York, 151 (1960).

Brooker, E. W., and H. O. Ireland, "Earth Pressures at Rest Related to Stress History," *Can. Geotech. J.*, **11**, 1 (1965).

Purchas, Derek, *Solid/Liquid Separation Technology*, Uplands Press Croydon, England, Ch. 5 (1981).

Shirato, M., T. Murase, and K. Kobayashi, "The Method of Calculation for Non-Unidimensional Filtration," *Filtration and Separation*, **5**, 219 (1968).

Shirato, M., and T. Aragaki. "The Relation Between Hydraulic and Compressive Pressures in Non-Unidimensional Filter Cakes," *Kagaku Kogaku*, **33**, 205 (1969).

Shirato, M., K. Kobayashi, and M. Tanimura, "Analysis of Constant Pressure Filtration of Compressible Cakes on Cylindrical Surface," *Kagaku Kogaku*, 37, 76 (1973).

Tiller, F. M., and H. R. Cooper, "The Role of Porosity in Filtration. V: Porosity Variation in Filter Cakes," *AIChE J.*, **8**, 445 (1962).

Tiller, F. M., and J. R. Crump, "Solid-Liquid Separation, An Overview," *Chem. Eng. Prog.* **73**, 65 (Oct., 1977).

Tiller, F. M., and W. M. Lu, "The Role of Porosity in Filtration. VIII: Cake Nonuniformity in Compression-Permeability Cells," *AIChE J.*, **18**, 569 (1972).

Tiller, F. M., and W. F. Leu, "Basic Data Fitting in Filtration," *J. Chinese Inst. Chem. Engr.*, **11**, 61 (1980).

Yoshioka, N., K. Ueda, and T. Hirao, "Study on Constant-Pressure Filtration Though Some Nonplane Filter Leaves," *Kagaku Kogaku*, **33**, 80 (1969).

Yoshioka, N., K. Ueda, and K. Miyoshi, "Liquid Pressure Distribution for Filtration Through Curved Leaves," *J Chem. Eng. Japan*, **5**, 291 (1972).

Manuscript received May 8, 1984; revision received Aug. 2 and accepted Oct. 29, 1984.